Proceedings of the 19th International Symposium on the Packaging and Transportation of Radioactive Materials
PATRAM 2019
August 4-9, 2019, New Orleans, LA, USA

$^{10}B(n, \alpha)^{7}Li$ Reaction-Assisted Corrosion of Al-B_4C Metal Matrix Composite Neutron Absorber Irradiated in Spent Nuclear Fuel Pool

Yunsong Jung
Ulsan National Institute of Science and Technology

Kiyoung Kim
Central Research Institute, Korea Hydro & Nuclear Power Co., Ltd

Sangjoon Ahn
Ulsan National Institute of Science and Technology

ABSTRACT

Al-B_4C metal matrix composites (MMC) are neutron absorber materials widely used in spent fuel pool (SFP) to ensure the subcriticality with more densely stored fuel assemblies. The performance and safety of the absorber material was experimentally demonstrated considering only low level irradiation assisted corrosion at a lukewarm temperature (20 ~ 49 °C) of the coolant, and then 40 years of service time was guaranteed. Recently, however, Korea Hydro & Nuclear Power Co., Ltd (KHNP) has discovered white spots from the surface of the surveillance coupons that have been submerged under a Korean SFP for 8 years and 3 months. This unexpectedly premature corrosion was not evident from the accelerated corrosion tests equivalent to 20 years of storage time in typical SFP without irradiation. We have been speculated that the radiation damage induced by $^{10}B(n, \alpha)^{7}Li$ reaction from boron-bearing particles, and also possibly from boron crud on the absorber surface, may have expedited the corrosion partially owing to ballistic atomic mixing and radiation-enhanced diffusivity, radiation-damaged porous surface, and locally elevated system temperature. In this study, the microstructures of various period-installed (33, 52, and 99 months) surveillance coupons were characterized. Highly radiation damaged structures such as numerous helium bubbles in aluminum matrix, microcracks in boron carbide, and correspondingly reduced density were commonly observed in all three period coupons. Since the severe microstructural evolution suggested potentially large boron depletion, the neutron transmission rates of the coupons were reevaluated by neutron attenuation test, which showed a stepwise reduction of the boron concentrations in the order of storage periods.

INTRODUCTION

Neutron absorbers are widely used in SFP and dry cask to ensure the subcriticality with more densely stored fuel assemblies. The qualification of the absorbers in SFP was experimentally demonstrated with the accelerated corrosion test and irradiation test considering only neutron

and gamma irradiation [1]. However, severe radiation damage induced by the $^{10}B(n, \alpha)^{7}Li$ could be concentrated at or near boron-bearing particles, which could lead to premature corrosion failure of neutron absorbers. Recently, the KHNP has discovered unexpectedly faster degradation, white spots, from the surface of surveillance coupons with reduced boron-10 areal density [2]. In this study, we characterized several-year irradiated Al-B_4C MMC from Hanul Unit 3 SFP and observed highly radiation damaged structure with the reduction of boron-10 concentration.

EXPERIMENTAL

Material

The Al-B_4C MMC is fabricated from high-purity aluminum 6061 and nuclear grade boron carbide powder (ASTM C750 Type 1) as shown in Table 1. The surveillance coupons (100 mm × 200 mm × 2.7 mm) of Al-32.4 wt% B_4C MMC for three different storage periods in Hanul Unit 3 SFP (2y9m: 2 years 9 months, 4y4m: 4 years 4 months, and 8y3m: 8 years 3 months) were received from KHNP. Table 2 shows the water chemistry condition and temperature in the SFP and acceptance criteria.

Table 1. The composition of Al-B_4C MMC [1]

Al 6061 powder		**ASTM C750 Type 1 B_4C powder**	
Element	**wt%**	**Element**	**wt%**
Al	Bal.	**B**	76.5 (Min.) (^{10}B :19.90 ± 0.3 at%)
Mg	0.08 ~ 1.2		
Si	0.4 ~ 0.8	**Si**	0.5
Cu	0.15 ~ 0.4		
Fe	0.15 (Max).	**Fe**	0.5
Zn	0.25 (Max.)		
Ti	0.15 (Max.)	**Ca**	0.3
Others	0.15 (Max.)		

Table 2. The water chemistry condition and temperature in Hanul Unit 3 SFP

	Hanul Unit 3 SFP	**Acceptance criteria**
Maximum water temperature (℃)	47.7	60
Boron concentration (ppm)	4,134	2,150 (Min.)
Lithium concentration (ppm)	0.6	2.5 (Max.)
Chlorine concentration (ppm)	1.5	150 (Max.)
Fluorine concentration (ppm)	1.7	150 (Max.)
Magnesium concentration (ppm)	1.1	250 (Max.)
pH	4.4	3.8 ~ 10.5

Characterization

Figure 1 shows as-received coupons sectioned into plates (5 mm × 5 mm × 2.7 mm) using a

waterjet to avoid adverse effects on microstructure [3]. The surface morphology was observed using a field-emission scanning electron microscopy (FE-SEM, FEI Quanta 200 FEG System) and micro-chemical analysis was carried out using an energy dispersive X-ray spectroscopy (EDS, Genesis 2000, EDAX). TEM specimens (7 μm × 5 μm × 100 nm) were prepared using focused ion beam (FIB, Helios 450HP, FEI) with the lift-out technique from the surface and characterized using a transmission electron microscope (TEM, JEM-2100F, JEOL).

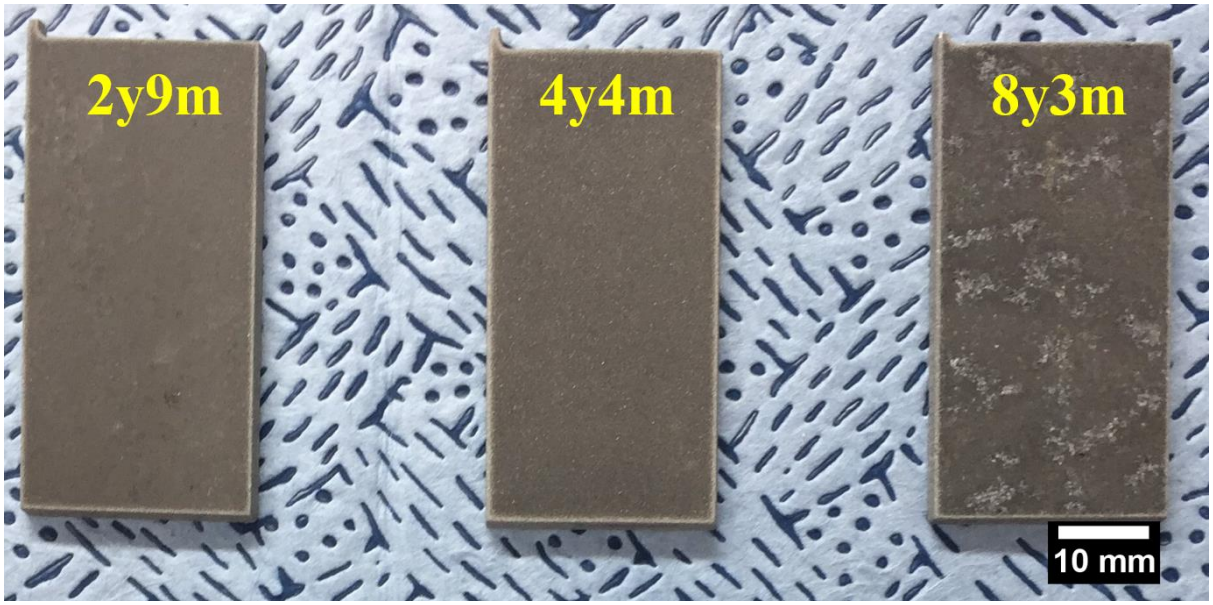

Fig. 1. As-received neutron absorber installed in Hanul Unit 4 SFP

Thermal neutron attenuation test

The thermal neutron field consists of ^{241}Am-Be neutron source, graphite moderator, He-3 detector, and cadmium thermal neutron filter. The thermal neutron transmission rate of neutron absorber was calculated using the equation (1).

$$P = \frac{S_t - S_e}{R_t - R_e} \times 100 \quad (1)$$

P : Thermal neutron transmission rate (%)
S_t : Count rate from the source with a coupon (cps)
S_e : Count rate from the source with a coupon and Cd cover (cps)
R_t : Count rate from the source (cps)
R_e : Count rate from the source with Cd cover (cps)

Density measurement

The density of neutron absorber was determined by the hydrostatic weighing in water. The

neutron absorbers were weighed by an electronic balance (AUX-220, Shimadzu) and the densities were calculated using the equation (2).

$$\rho = \frac{m_{air}}{m_{wet} - m_{water}} \times \rho_{water} \quad (2)$$

ρ : The density of neutron absorber (g/cm^3)
ρ_{water} : The density of water (g/cm^3)
m_{air} : The mass of the neutron absorber in the air (g)
m_{wet} : The mass of the water-impregnated neutron absorber in the air (g)
m_{water} : The mass of the neutron absorber in water (g)

RESULTS AND DISCUSSION

Microcracks and pit in boron carbide

Surface degradation of boron carbide particles was observed for all three period specimens as shown in Figs. 2 and 3. Microcracks were formed in boron carbide which may channel the release of helium gas from the $^{10}B(n, \alpha)^7Li$ reaction [4]. Figure 3 shows smalls pits in boron carbide that can lead to the potential loss or redistribution of boron-10 loss.

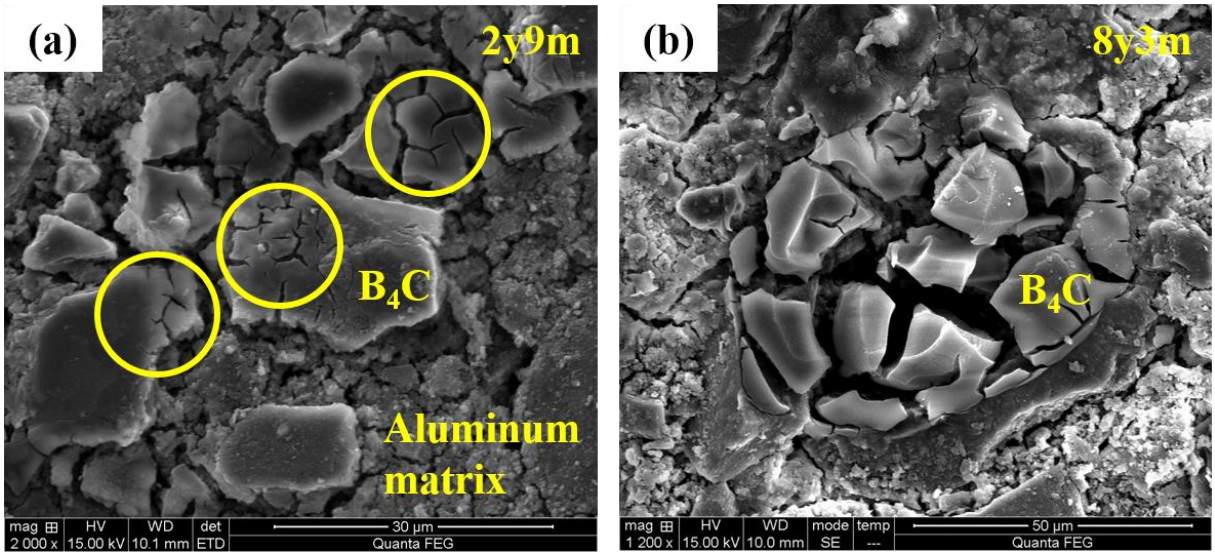

Figure 2. The microcracks in 2y9m (a), 8y3m (b)

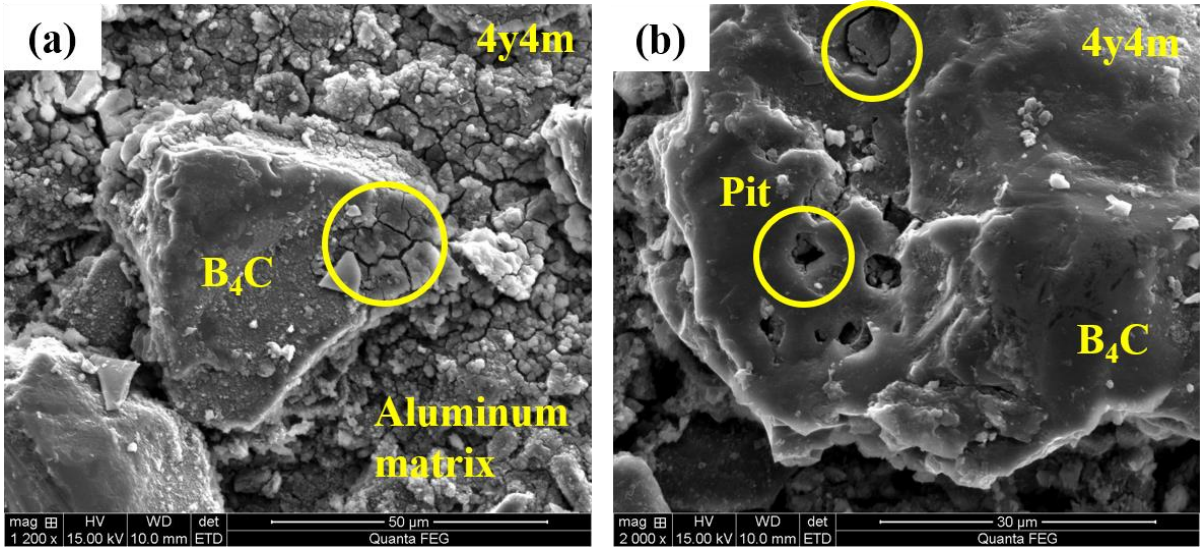

Figure 3. The microcracks (a) and pits (b) in 4y4m

Helium bubble formation in aluminum matrix

Figure 4 shows numerous helium bubble formed near B_4C particles in the aluminum matrix of 8y3m by the $^{10}B(n, \alpha)^7Li$ reaction. Average and maximum bubble diameters were estimated as 27 nm and 57 nm by using ImageJ software (National Institutes of Health). Based on the premature corrosion failure of surveillance coupons and the highly damaged aluminum matrix, energetic α-particles (~1.5 MeV) and lithium ions (~0.8 MeV) emitted from the $^{10}B(n, \alpha)^7Li$ reaction could have expedited the corrosion of neutron absorbers partially owing to ballistic atomic mixing and radiation-enhanced diffusivity, radiation-damaged porous microstructure, and locally elevated system temperature.

Reduced density of neutron absorbers

Figure 5 show monotonically decreasing density of neutron absorbers following the increasing irradiation time in the SFP; relative density reduction rate was more or less constant for all three periods, ~0.04% per month. This decreasing trend of absorber density, likely attributed to helium bubble formation and growth, reflects porous microstructure of the absorber after being irradiated, which may expedite the corrosion of the material.

Boron-10 depletion

Since the severe microstructural evolution suggested potentially large boron depletion, thermal neutron attenuation tests of 16 coupons (2y9m: 4, 4y4m: 6, and 8y3m: 6) were performed. The boron-10 areal density of pre-irradiated coupons was 0.0335 ± 0.0005 g/cm^2. The boron-10 depletion was estimated with the shortest exposed coupon since no as-fabricated coupon was provided from the manufacturer. After 19 months, 3.4 % of boron-10 was depleted and 47 months later, 11.5 %, as shown in figure 5. Compared with the exponential fitted transmission rate of pre-irradiated coupons, 4.6% and 12.6 % of boron-10 were depleted.

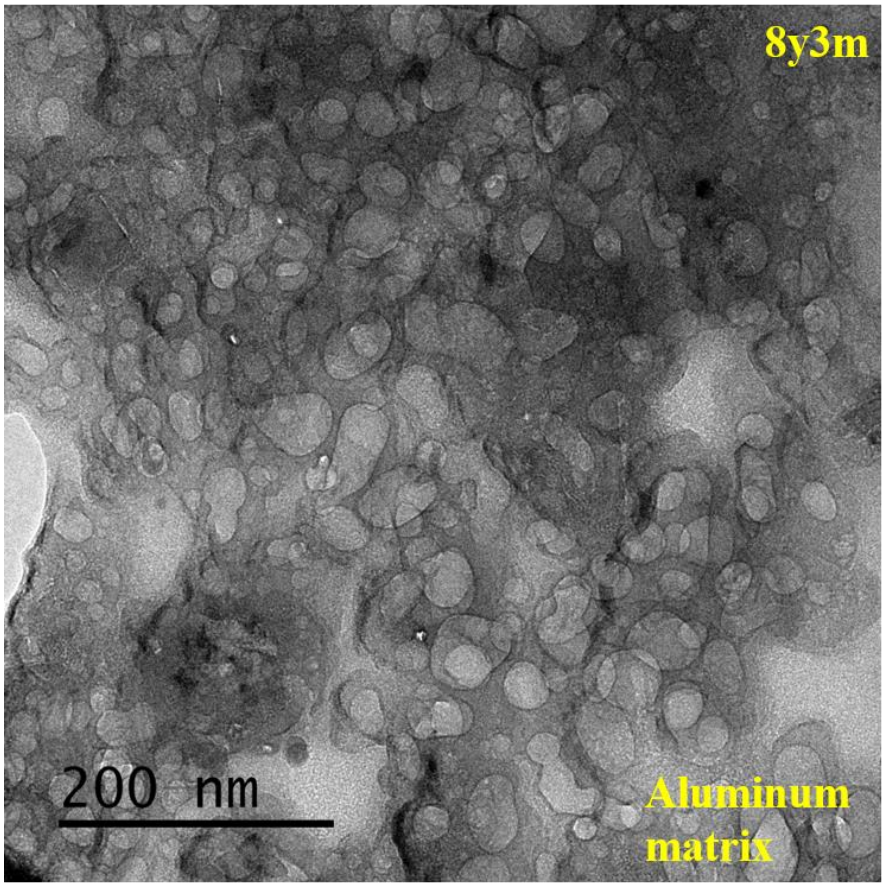

Figure 4. Numerous helium bubble formation in aluminum matrix of 8y3m

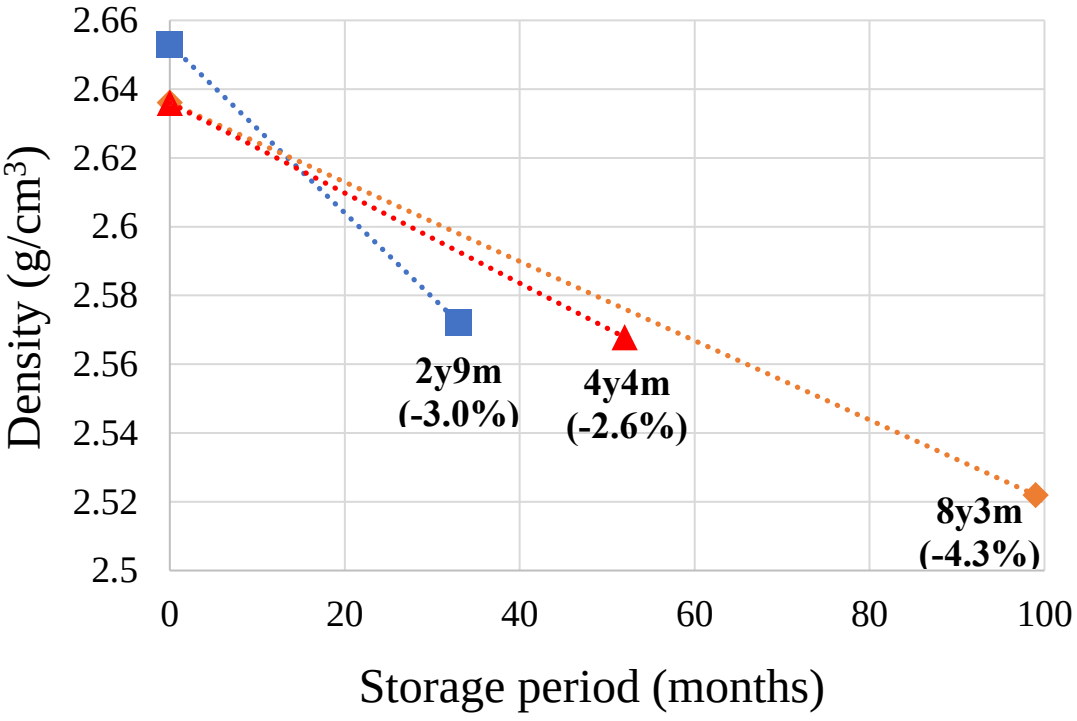

Figure 5. Reduced density of neutron absorbers depending on the storage period

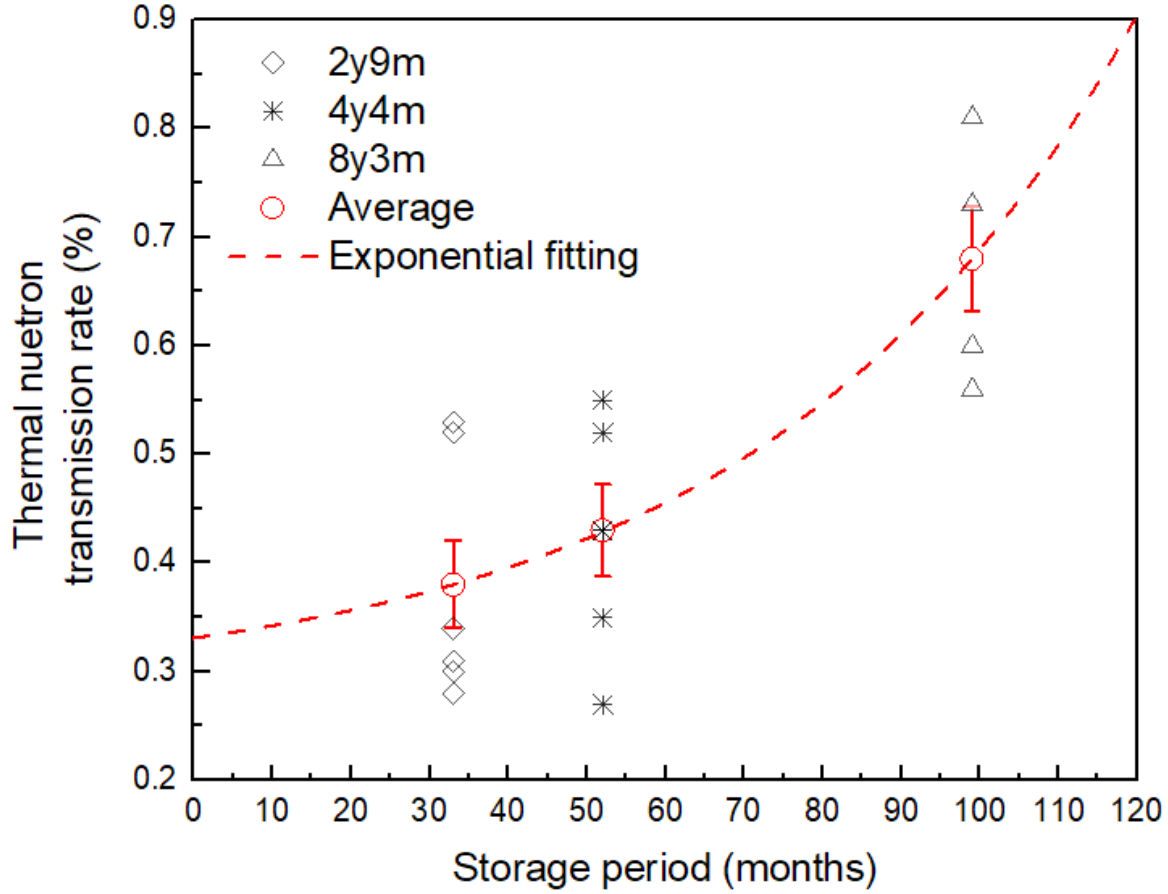

Figure 6. The thermal neutron transmission rate of neutron absorbers

CONCLUSIONS

Microstructures of various period-installed (33, 52, and 99 months) neutron absorber surveillance coupons from Hanul Unit 3 spent fuel pool were investigated in regard to recently found white spots on B_4C bearing Al-based neutron absorber surface. Significantly radiation damaged microstructures, such as numerous helium bubbles, B_4C particle microcrack and pits, perhaps due to energetic helium and lithium ions emitted from $^{10}B(n, \alpha)^7Li$ reaction, were observed with corresponding density reduction at ~0.04% per month rate. Porous absorber surface combined with irradiation effects, accounting the neutron-induced particle emission reaction, may have accelerated the premature corrosion of the neutron absorber in SFP to form the white spot. Thermal neutron attenuation test on the surveillance coupons was conducted to assess the degree of boron-10 depletion rate, concerning possibly expedited boron depletion rate, which was estimated as 11.5% for 47 months in the SFP.

ACKNOWLEDGMENTS

This work was supported by Korea Hydro & Nuclear Power Co., Ltd (2017-Tech-18).

REFERENCES

[1] Qualification of METAMIC® For Spent-Fuel Storage Application, EPRI, Palo Alto, CA: 2011, 1003137.

[2] K. Kim, S. Chung, J. Hong, Performance Evaluation of METAMIC Neutron Absorber in Spent Fuel Storage Rack, Nuclear Engineering and Technology, Vol. 50, pp. 788, 2018.

[3] A. Akkurt, The Effect of Cutting Process on Surface Microstructure and Hardness of Pure and Al 6061 Aluminium alloy, Engineering Science and Technology, an International Journal, Vol. 18, pp. 303, 2015.

[4] A. Inoue, T. Onchi, Irradiation Effects of Boron Carbide Used as Control Rod Elements in Fast Breeder Reactors, Journal of Nuclear Materials, Vol. 74, pp. 114, 1978.